Available online at www.sciencedirect.com

ScienceDirect

journal homepage: www.elsevier.com/locate/he

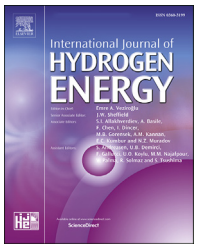

A new biomass gasification driven hybrid system for power and liquid hydrogen cogeneration: Parametric study and multi-objective evolutionary optimization

Haitao Lin [a], *Xianhua Wu* [a,*], *Hamdi Ayed* [b,c], *Abir Mouldi* [d], *Syed Zaheer Abbas* [e], *Amir Ebrahimi-Moghadam* [f,**]

[a] *Yuxi Normal University, Yunnan Province, ZIP 653100, China*
[b] *Department of Civil Engineering, College of Engineering, King Khalid University, Abha, 61421, KSA*
[c] *Higher Institute of Transport and Logistics of Sousse, University Sousse, Sousse 4023, Tunisia*
[d] *Department of Industrial Engineering, College of Engineering, King Khalid University, Abha, 61421, KSA*
[e] *Department of Mathematics & Statistics Hazara University Mansehra Pakistan*
[f] *Mechanical Engineering Department, Faculty of Engineering, Ferdowsi University of Mashhad, Mashhad, Iran*

HIGHLIGHTS

- Optimizing proposed system is determined.
- The subsystems are biomass unit, SRC, and PEM electrolyzer.
- Tri-objective optimization and economic analyses are applied.

ARTICLE INFO

Article history:
Received 9 December 2021
Received in revised form
6 January 2022
Accepted 13 January 2022
Available online 18 February 2022

Keywords:
Biomass-fueled gas turbine cycle
Rankine cycle
Hydrogen liquefaction cycle
Exergoeconomic analysis
NSGA-II optimization

ABSTRACT

The purpose of this paper is focused on introducing a new layout of an electricity and liquid hydrogen cogeneration power plant and evaluating its performance from the exergo-economic and environmental stand points. The system is based on the combination of a biomass gasification gas turbine cycle, a Rankine cycle, an electrolyzer unit, and a hydrogen liquefaction cycle. A parametric model is firstly developed to study the sensitivity of the system performance on the main design parameters (including biomass flow rate $\dot{m}_{biomass}$, gas turbine inlet temperature T_{GT}, compressor pressure ratio PR, and steam turbine inlet pressure P_{SRCT}). Afterward, the optimal operation of system is selected using by a multi-objective optimization approach. The observations revealed that $\dot{m}_{biomass}$ is the most effective design parameter. The optimal design parameters are obtained as $\dot{m}_{biomass}$ = 1.94 kg/s, T_{GT} = 1421 K, PR = 5.52, and P_{SRCT} = 3886 kPa, which results in the maximum electricity and hydrogen production of 3377 kW and 14.8 kg/h together with minimum total cost rate of 86.61 $/h. At this condition, the optimal environmental index is 1.09 kg_{CO_2}/kWh.

* *Corresponding author.*
** *Corresponding author.*
E-mail addresses: xhw105@yxnu.edu.cn (X. Wu), amir_ebrahimi_051@yahoo.com (A. Ebrahimi-Moghadam).
https://doi.org/10.1016/j.ijhydene.2022.01.110

Nomenclature

G^0	Molar Gibbs free energy, J/mol
K	Equilibrium constant
T	Temperature, K, C
$\overline{h}_f^0$	Enthalpy of formation, kJ/kmol
S	Specific entropy, kJ/kmol K
$\dot{Q}$	Heat rate, kW
$\dot{m}$	Mass flow rate, kg/s
H	Specific enthalpy, kJ/kg
$\dot{W}$	Power, kW
$\dot{E}x$	Exergy rate, kW
R	Universal gas constant, J/mol K
ex_{Ch}	Standard molar chemical exergy, kJ/mol
$\dot{Z}$	Capital cost rate, $/h
N	Component lifetime
i_{eff}	Interest rate
CRC	Cost recovery coefficient

Abbreviations

HPP	Hybrid power plant
GTC	Gas turbine cycle
WHR	Waste heat recovery
ORC	Organic Rankine cycle
ERC	Ejector refrigeration cycle
PEMEC	Proton exchange membrane electrolyzer cycle
FC	Fuel cell
GA	Genetic algorithm
KC	Kalina cycle
CCHP	Combined cooling, heating and power
SRC	Steam Rankine cycle

Greek symbol

ζ	CO_2 emission, kg/kWh
Δ	Difference
η	Efficiency, %

Introduction

In the last decades, different factors leads to creation of a unanimous sense in the human that there is serious need of increasing the share of renewable resources in the global energy matrix [1–3]. These factors are mainly related to defects of conventional primary energies [4] and forced the governments to invest in different areas of generating/storing renewable-based energies [5]. From some of important these factors it could be mentioned to the limitation in reserves of conventional primary energies, significant reliance of the current power plants on them, and their environmental damages [6,7]. Although the renewable resources have numerous benefits, their unpromising due to climatic changes and other natural constraints are their big shortcomings. In most cases, the bioenergy solves these deficiencies [8] and this makes it as one of the most widely-used renewable resources in power plants (through direct firing of biomass or the combustion of syngas produced from biomass).

Producing/storing clean sustainable energies through efficient instrument has become one of the prominent issues. In this regard, hydrogen production through waste heat recovery (WHR) approach in hybrid power plants (HPPs) is a trend topic in the field of study. In HPPs there possibility of producing different kinds of energies (electricity, heat, and cold) [9,10], hydrogen [11], freshwater [12], etc. in an integrated system. The configuration of such system is made of a prime mover cycle and some bottoming cycles. Among different cycles, the gas turbine cycle (GTC) is known as one of the conventional power cycles which has widely been utilized as a mover cycle due to its high heating potential in deriving some bottoming cycles through WHR from its exhaust gases. Also, the Rankine cycle (RC) and its organic version (known as ORC), Kalina cycle (KC), ejector refrigeration cycle (ERC), multi-effect desalination (MED) unit, proton exchange membrane electrolyzer cycle (PEMEC), etc. have widely been employed as bottoming cycles for producing different kinds of energies.

In one the most recent published works in this concept, Wang et al. [13] performed a comprehensive study around a novel HPP producing power, heat, and cold simultaneously. They developed a robust techno-economic-environmental model and applied an evolutionary multi-criteria optimization approach. They presented the values of 106.04 €/kW 9.36 kg/kW as the optimal annual values of eco-environmental indices. Ebrahimi-Moghadam and Farzaneh-Gord [14] designed a CHP + H_2 trigeneration plant for using in natural gas industry. The produced heat was used for natural gas preheating and the hydrogen was fed to natural gas pipelines. Hence, their proposal could be considered as an application of power-to-gas technology. Ebrahimi-Moghadam et al. [15] evaluated the performance of combining three bottoming cycles (including an RC, an ERC, and a PEMEC) with a RGTC (as prime mover cycle). They utilized energy, exergy, exergo-economic, and exergo-environmental analyses for this evaluation. The system's outputs was included 21.42 MW of power, 26.81 MW of heating, 8.89 MW of cooling, and 11.96 kg/h of hydrogen. Altinkaynak and Ozturk [16] introduced a new CCHP (combined cooling, heating and power)+H_2 multi-generation system through coupling of two types of GTC, two types of RC, an ejector refrigeration cycle, and a hydrogen production/storage unit. They accomplished the thermodynamics analyses to evaluate their proposal and obtained the energetic and exergetic efficiencies of 44.69% and 42.03%, respectively. Ebrahimi-Moghadam et al. [17] developed comprehensive exergo-economic and exergo-environmental models of a CCHP district energy system. They coupled artificial intelligence and genetic algorithm (GA) optimization approaches and reached to optimum primary ratio of 76.9%. Ding et al. [18] sought the optimal operation of a power and freshwater cogeneration system. The system comprised of a regenerative GTC (RGTC), a KC, and a HD desalination unit. They considered exergetic efficiency and levelized total emission as optimization objective functions and found their optimum value as 0.4384 and 62,602 kg/kW, respectively. Ahmadi et al. [19] proposed a HPP producing electricity, heat,

and freshwater. The system layout was based on WHR from a GTC by utilizing a HRSG (heat recovery steam generator) to run a MED-TVC unit. Ebrahimi-Moghadam et al. [20] performed a comprehensive thermodynamics-based sensitivity analysis to investigate the effects of some key parameters in a CCHP HPP. The system comprised a RGTC, a KC, and an ejector refrigeration cycle. Their results illustrated that the KC has low exergy destruction.

Over the past decades, the global energy matrix insist on the use of renewable energy resources in the energy production sectors, which leads to have cleaner productions. The use of solar- and bio-driven/assisted GTCs has attracted the attentions of researchers in design of novel clean HPPs. In this concept, Alirahmi et al. [21] sought the optimal design conditions of a system with the ability of producing and storing energy. The system was based on the combination of a solar-driven GTC, a RC, a PEME hydrogen production unit, and a CAES (compressed air energy storage) system. They applied their investigations on Los Angeles (as case study) and reached to 3313 ton/year CO_2 release reduction. Al-Hamed and Dincer [22] introduced a new multigeneration energy system which uses natural gas and solar radiation as prime running energy sources. They developed thermodynamics model of their proposal and found that solar irradiance has a significant effect on the system efficiency. Musharavati et al. [23] analyzed a syngas-fired cogeneration system which generates electricity and freshwater. They combined artificial intelligence and grey-wolf optimization approaches demonstrated that total cost rate is 206.78 $/h in their proposal. Cao et al. [24] introduced a new configuration of a hybrid power generation system which was built by the combination of a biomass-solar driven GTC with hydrogen post-firing, a RC, and a PEME unit. Applying the GA (genetic algorithm) optimization method, they reached to minimum electricity cost of 61.37 $/MWh and CO_2 emission of 0.4579 kg/kWh. In another work, Alirahmi et al. [25] recovered the wasted heat of a biomass-fueled solar-assisted GTC to run four sub-systems for producing power, freshwater, and hydrogen. They proposed a robust optimization approach aiming the maximization of exergetic efficiency and minimization of cost rate, simultaneously. They found the optimal objective functions as 26.7% and 224.1 $/h. Wang et al. [26] designed a new layout of a cooling, heating, and power trigeneration system based on the WHR from a solar-assisted GTC to run a DWH (domestic water heater) and a cooling/heating absorption cycle. Their results showed that the energetic efficiency of the system is respectively 83.6% and 66% in the cooling and heating modes. Karimi et al. [27] applied the WHR approach to exhaust gases of a GT-SOFC cycle for generating some additional power in an ORC. At the optimum conditions, their proposed CHP system generated 329 kW and 56 kW of power and heat, respectively. Nazari and Porkhial [28] developed exergo-economic model and optimization of a CCHP + freshwater multigeneration energy system. The system was composed of a solar-assisted biomass-fired GTC, two RCs (including steam and organic RCs), an ARC, and a MED unit. The findings demonstrated that using natural gas instead of their studied biomass leads to around 3 times increment in system's total production costs (for a same system outputs). Shokouhi Tabrizi et al. [29] studied feasibility of using a solar-based heat and power cogeneration plant in natural gas industry. Their model consists of thermodynamics and economic principles and they concluded the payback period time is around 8 years based on NPV (net present value) method.

Designing new eco-friendly HPPs based on the renewable resources is an interesting topic which have attracted many attentions in recent years. Relying on the available literature, hydrogen is a clean fuel for near future and HPPs with hydrogen production/storage units are under developing. Also, the liquid hydrogen is the cleanest natural fuel which limited researches have been conducted to produce it in HPPs. On the other side, reviewing the available literature states that limited researches have been conducted around the use of hydrogen liquefaction cycles in the HPPs. In this context, most of the previous papers have investigated only hydrogen gas production and limited studies paid to modeling of the liquefaction process after hydrogen production. Therefore the necessity to such systems is still sensed in the field of study. Hence, to address this gap, the following objectives/novelties are sought in this study:

- Presenting a novel enviro-friendly HPP for simultaneous production of the electricity and liquid hydrogen. For this, a biomass-fueled GTC is considered as the mover cycle and the Linde-Hampson cycle is used for liquefaction process.
- A detailed computational model is developed based on the 4E (energy, exergy, exergo-economic, and environmental) principles and the effect of system's key parameters on the assessment indices is studied applying a parametric study.
- Finally, the system's optimal operating condition is found using by a robust optimization procedure based on the combination of artificial neural network (ANN) and NSGA-II (non-dominated sorting genetic algorithm) optimization method.

Description of the system under investigation

Fig. 1 shows the proposed schematic of the biomass gasification plant. The system includes three subsystems: biomass unit, steam Rankine cycle (SRC), and hydrogen liquefaction unit. As shown in Fig. 1, ambient air enters the gasifier as a gasification agent after being compressed. Afterward, the syngas produced in the gasifier enters the combustion chamber and react with compressed air from compressor 1. Combustion products with high temperatures are expanded in the gas turbine to produce power.

The exhaust gases from the gas turbine still have a high temperature, so SRC is utilized to restore the heat. Next, the generated electric power by SRC is transferred into an electrolyzer to produce hydrogen and oxygen. The introduced HPP utilizes a PEME unit. The main benefits of the PEMEs over alkaline and solid oxide electrolyzers are fast system response, high current density, commercialization potential, and high voltage efficiency.

The produced hydrogen is then compressed by a compressor. The high-pressure hydrogen is split into two flows. The hydrogen gas in recuperator 1 is cooled using cold hydrogen vapor returning from the liquid hydrogen reservoir. The remaining stream is passed through recuperator 2 in

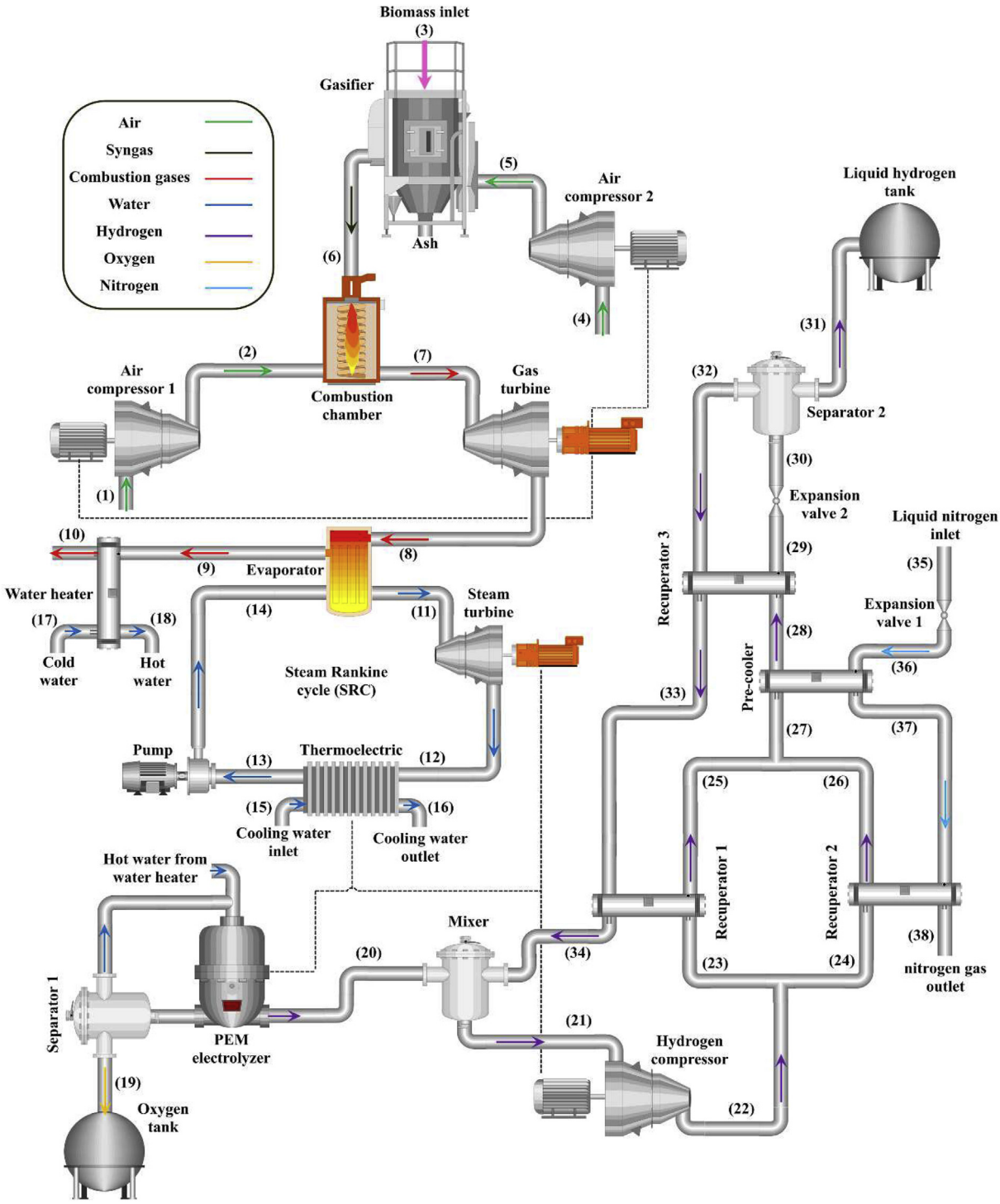

Fig. 1 – Schematic diagram of the proposed system to produce liquid hydrogen and power.

which is cooled using returning nitrogen vapor from a pre-cooler. The hydrogen flows are then combined and enter the pre-cooler. Next, the hydrogen passes through the recuperator 3, cooled by hydrogen vapor from a liquid hydrogen reservoir. The high-pressure hydrogen egressing the recuperator 3 passes through the hydrogen throttle valve and is transformed into a two-phase state. Then the liquid hydrogen is separated from the hydrogen vapor and stored in special storage. The cycle represented in Fig. 1 includes a typical Linde-Hampson stage and a pre-cooler stage that consumes the liquid nitrogen.

Mathematical formulation

As mentioned, the problem under investigation is focused on the evaluation of the introduced HPP from energy, exergy, exergo-economic, and environmental points-of-view. Finally,

the optimal operation of the proposal is found through a multi-objective optimization approach. Hence, the objective of this section is focused on presenting details of these procedures.

Energy analysis

The energetic model is based on the firs-law of thermodynamics. The final form of the energy balance equation for steady state conditions is expressed as Eq. (1). As can be inferred from this equation, calculating thermo-physical properties of all flow streams is required for developing the energetic model. Furthermore, the mass flow rate of flow streams should be determined by applying the continuity equation (Eq. (2)) [30].

$$\left(\sum_{in}\left[\dot{m}\left(h+\frac{u^2}{2}+gz\right)\right]_{in,k}\right)+\sum\dot{Q}_k=\left(\sum_{out}\left[\dot{m}\left(h+\frac{u^2}{2}+gz\right)\right]_{out,k}\right)+\sum\dot{W}_k \tag{1}$$

$$\sum_{in}\dot{m}_{in,k}=\sum_{out}\dot{m}_{out,k} \tag{2}$$

In the above equations, the parameters of $\dot{m}$, h, u, g, and z stand for mass flow rate, specific enthalpy, velocity, gravity acceleration, and height of the flow streams in the system.

It is worth mentioning that some of the system components need some auxiliary formula to develop those energetic model. In the system under investigation, these components are included gasifier, combustion chamber, and electrolyzer.

Gasifier

As noted before, utilizing a gasifier, the biomass is firstly converted to syngas which is then used as the fuel in combustion chamber of GTC. The gasifier is composed of four zones including drying, pyrolysis, combustion (shift reaction), and reduction (methanation reaction). The reaction within each of these zones is assumed to be occurred in thermodynamics equilibrium and written as the following equations [31]:

$$C+CO_2\leftrightarrow 2CO \tag{3}$$

$$C+H_2O\leftrightarrow CO+H_2 \tag{4}$$

$$CO+H_2O\leftrightarrow CO_2+H_2 \tag{5}$$

$$C+2H_2\leftrightarrow CH_4 \tag{6}$$

For predicting the composition of the syngas, the general form of the gasification reaction for a biomass with general chemical formula of $CH_aO_bN_c$ is written as follows [32]:

$$CH_aO_bN_c+n_{H_2O}H_2O+n_{air}(O_2+3.76N_2)\rightarrow n_1H_2+n_2CO+n_3CO_2+n_4H_2O+n_5CH_4+n_6N_2 \tag{7}$$

where, n_{H_2O} shows the biomass moisture content (is determined using Eq. (8)) and n_{air} is the amount of inlet air (kilomoles of air per kilomoles of biomass). Also, the six coefficients of n_1 to n_6 can be determined with applying the molar balance for carbon, hydrogen, oxygen, and nitrogen in the gasification reaction (are written in Eq. (9)) and also using the methanation and shift reactions equilibrium constants (are defined based on Eq. (10)) [33,34]. In the present work, the wood is considered as the biomass.

$$MC=\frac{\text{mass of water}}{\text{mass of wet biomass}}\times 100=\frac{18n_{H_2O}}{M_{biomass}+18n_{H_2O}}\times 100\Rightarrow n_{H_2O}=\frac{M_{biomass}\times MC}{18\times(1-MC)} \tag{8}$$

$$\begin{cases} Carbon\ balance: n_2+n_3+n_5=1 \\ Hydrogen\ balance: 2n_1+2n_4+4n_5=a+2n_{H_2O} \\ Oxygen\ balance: n_2+2n_3+n_4=b+n_{H_2O}+2n_{air} \\ Nitrogen\ balance: 2n_6=c+(3.76\times 2n_{air}) \end{cases} \tag{9}$$

$$\begin{cases} K_{MR}=\dfrac{P_{CH_4}}{(P_{H_2})^2}=exp\left(-\dfrac{\Delta G^0_{MR}}{RT_g}\right) \\ K_{SR}=\dfrac{P_{CO_2}\times P_{H_2}}{P_{CO}\times P_{H_2O}}=exp\left(-\dfrac{\Delta G^0_{SR}}{RT_g}\right) \end{cases} \tag{10}$$

where, the parameters of MC, $M_{biomass}$, ΔG^0_{MR}, ΔG^0_{SR}, R, and T_g are the moister content per mole of biomass, the biomass molecular weight, change in the standard Gibbs free energy of the reactions, the universal gas constant, and the gasifier temperature, respectively.

Finally, the energy balance equation for the gasifier is presented as:

$$\begin{aligned}\bar{h}^0_{f,biomass}+n_{H_2O}\times\bar{h}^0_{f,H_2O}=&\ n_1\left(\bar{h}^0_{f,H_2}+\Delta\bar{h}_{H_2}\right)+n_2\left(\bar{h}^0_{f,CO}+\Delta\bar{h}_{CO}\right)\\&+n_3\left(\bar{h}^0_{f,CO_2}+\Delta\bar{h}_{CO_2}\right)+n_4\left(\bar{h}^0_{f,H_2O}+\Delta\bar{h}_{H_2O}\right)\\&+n_5\left(\bar{h}^0_{f,CH_4}+\Delta\bar{h}_{CH_4}\right)+n_6\left(\bar{h}^0_{f,N_2}+\Delta\bar{h}_{N_2}\right)\end{aligned} \tag{11}$$

Combustion chamber

A complete combustion reaction between the produced syngas in the gasifier and the compressed air from compressor is occurred within the combustion chamber, which is written as Eq. (12). Also, the energy balance equation for the combustion chamber is described as Eq. (13).

$$(n_1H_2+n_2CO+n_3CO_2+n_4H_2O+n_5CH_4+n_6N_2)+n_{air}(O_2+3.76N_2)\rightarrow n_1H_2+n_2CO+n_3CO_2+n_4H_2O+n_5CH_4+n_6N_2 \tag{12}$$

$$\sum\left[n\left(\bar{h}^0_f+\Delta\bar{h}\right)\right]_{\text{gasifier's produced gases}}+\sum\left[n\left(\bar{h}^0_f+\Delta\bar{h}\right)\right]_{air}=\sum\left[n\left(\bar{h}^0_f+\Delta\bar{h}\right)\right]_{products} \tag{13}$$

Electrolyzer

The electrolysis operation is established based on the water splitting reaction into its constituents, as expressed in Eq. (14). In this equation, the total needed energy of the splitting reaction is acquired based on the Gibbs free energy definition (Eq. (15)) [35].

$$H_2O+energy\rightarrow H_2+\frac{1}{2}O_2;\ \begin{cases} H_2O\rightarrow 2H^++2e^-+\frac{1}{2}O_2,\ Anode\ side \\ 2H^++2e^-\rightarrow H_2,\ Cathode\ side \end{cases} \tag{14}$$

$$\Delta G=\Delta H-T\Delta S \tag{15}$$

where, the parameters of G, H, and S respectively denotes the Gibbs free energy, enthalpy, and entropy, and the term $T\Delta S$ refers to the needed thermal energy.

The hydrogen's molar flow rate ($\dot{N}_{H_2}$) and required input power to the electrolyer unit ($\dot{W}_{PEME}$) can be calculated using the following equations, respectively [36].

$$\dot{N}_{H_2} = \frac{J}{2F} \tag{16}$$

$$\dot{W}_{PEME} = JV \tag{17}$$

In the above equations, J and F represents current density and Faraday constant, respectively. Also, V represents the voltage potential of the electrolyzer which is expressed as follows [37]:

$$V = V_0 + V_{act,a} + V_{act,c} + V_{ohm} \tag{18}$$

where, the required parameters for the determination of V is tabulated in Table 1:

Other system components

As the energy model of the other system components does not include additional formulation, the final simplified form of the energy balance and auxiliary equations of them are summarized in Table 2.

As one energetic technical assessment index, the net generated power of the system under investigation is defined as follows:

$$\dot{W}_{net} = \dot{W}_{GT} + \dot{W}_{ST} + \dot{W}_{TEG} - \dot{W}_{COMP_1} - \dot{W}_{COMP_2} - \dot{W}_{COMP_3} - \dot{W}_{PU} \tag{36}$$

Exergetic and exergo-economic governing equations

The main defect of the analysis based on the first-law of thermodynamics is that it does not considered the content which is destroyed during energy conversion processes (it just pays attention to the fact that the energy is converted from one form to the other forms, without any creation or destruction). But in the reality, something is lost during energy conversion reactions. To cover this deficiency, the second-law of thermodynamics should be utilized. The concept of exergy, representing the highest achievable amount of work within the processes, is defined in the second-law of thermodynamics. The rate of destroyed exergy ($\dot{\Psi}_k$) in component k during a process is expressed as [40]:

$$\dot{\Psi}_k = \left(\sum\nolimits_{in} \dot{E}x_{in,k}\right) - \left(\sum\nolimits_{out} \dot{E}x_{out,k}\right) + \left(\sum \dot{E}x_{Q,k}\right) - \left(\sum \dot{E}x_{W,k}\right) \tag{37}$$

where, the parameters of $\dot{E}x_{Q,k} = \left[1 - \frac{T_0}{T_k}\right]\dot{Q}_k$ and $\dot{E}x_{W,k} = \dot{W}_k$ respectively refers to the exergy rate due to heat transfer and work. Also, in this equation, each of the inlet and outlet exergy rates (i.e. $\dot{E}x_{in,k}$ and $\dot{E}x_{out,k}$) are composed of two terms including physical + chemical exergies, and can be obtained using the following equation [41]:

$$\dot{E}x_k = \overbrace{[\dot{m}((h - h_0) - T_0(s - s_0))]_k}^{\dot{E}x_{ph,k}} + \overbrace{\left[\dot{m}\left(\sum\nolimits_i Y_i ex_{Ch,i} + \overline{R}T_0 \sum\nolimits_i Y_i \ln Y_i\right)\right]_k}^{\dot{E}x_{ch,k}} \tag{38}$$

where, s is specific entropy, ex is specific exergy, and subscript "0" illustrates the reference thermodynamic conditions ($T_0 = 298$ K and $P_0 = 1.01$ bar).

By utilizing Eq. (37) and applying mathematical simplification operations, the final format of the exergy destruction rate for all of the system components is tabulated in Table A1 in Appendix A. Also, as one exergetic technical assessment index, the net generated power of the system under investigation is defined as follows:

$$\eta_{ex} = \frac{\dot{W}_{net} + \dot{E}x_{18} + \dot{E}x_{Liquid\ hydrogen}}{\dot{E}x_{biomass} + \dot{E}x_{35}} \tag{39}$$

Table 1 – Details of the required parameters for calculating the electrolyzer's voltage potential [38,39].

Item and equation	Remark
Reversible potential (the Nernst equation): V_0 $V_0 = 1.229 - [8.5 \times 10^{-4}(T_{PEME} - 298)]$	T_{PEME} is inlet temperature of electrolyzer.
Activation over-potential of the anode: $V_{actv,a}$ $V_{actv,a} = \frac{RT}{F}\sinh^{-1}\left(\frac{J}{2J_{0,a}}\right)$; $J_{0,a} = J_{ref,a}\exp\left(-\frac{E_{actv,a}}{RT}\right)$	$J_{0,a}$ and $E_{actv,a}$ are pre-exponential factor and activation energy of the anode.
Activation over-potential of the cathode: $V_{actv,c}$ $V_{actv,c} = \frac{RT}{F}\sinh^{-1}\left(\frac{J}{2J_{0,c}}\right)$; $J_{0,c} = J_{ref,c}\exp\left(-\frac{E_{actv,c}}{RT}\right)$	$J_{0,c}$ and $E_{actv,c}$ are pre-exponential factor and activation energy of the cathode.
Ohmic over-potential of the electrolyte: V_{ohm} $V_{ohm} = JR_{PEME}$ $R_{PEME} = \int_0^D \frac{dx}{\sigma_{PEME}(\lambda(x))}$ $\sigma_{PEME}(\lambda(x)) = [0.5139\lambda(x) - 0.326] \times exp\left[1268\left(\frac{1}{303} - \frac{1}{T_{PEME}}\right)\right]$ $\lambda(x) = \left(\frac{\lambda_a - \lambda_c}{D}\right)x + \lambda_c$	R_{PEME}, σ_{PEME}, D and λ_a and λ_c are overall resistance, local ionic conductivity, membrane thickness, and membrane anode and cathode surface water.

Table 2 – The energy balance formula for some of the cycles' components.

Component	Equation	Equation no.
Compressor 1	$\dot{W}_{COMP_1} = \dot{m}_1(h_2 - h_1)\ ;\ \eta_{COMP_1} = \frac{h_{2,s} - h_1}{h_2 - h_1}$	(19)
Compressor 2	$\dot{W}_{COMP_2} = \dot{m}_4(h_5 - h_4)\ ;\ \eta_{COMP_2} = \frac{h_{5,s} - h_4}{h_5 - h_4}$	(20)
Gas turbine	$\dot{W}_{GT} = \dot{m}_7(h_7 - h_8)\ ;\ \eta_{GT} = \frac{h_7 - h_8}{h_7 - h_{8,s}}$	(21)
Evaporator	$\dot{m}_8(h_8 - h_9) = \dot{m}_{14}(h_{11} - h_{14})$	(22)
Steam turbine	$\dot{W}_{ST} = \dot{m}_{11}(h_{11} - h_{12})\ ;\ \eta_{ST} = \frac{h_{11} - h_{12}}{h_{11} - h_{12,s}}$	(23)
Thermoelectric generator	$\dot{m}_{15}h_{15} + \dot{m}_{12}h_{12} = \dot{m}_{16}h_{16} + \dot{m}_{13}h_{13} + \dot{W}_{TEG}$	(24)
Pump	$\dot{W}_{PU} = \dot{m}_{13}(h_{14} - h_{13})\ ;\ \eta_{PU} = \frac{h_{14,s} - h_{13}}{h_{14} - h_{13}}$	(25)
Domestic water heater	$\dot{m}_{17}(h_{18} - h_{17}) = \dot{m}_9(h_9 - h_{10})$	(26)
Compressor 3	$\dot{W}_{COMP_3} = \dot{m}_{21}(h_{22} - h_{21})\ ;\ \eta_{COMP_3} = \frac{h_{22,s} - h_{21}}{h_{22,a} - h_{21}}$	(27)
Recuperator 1	$\dot{m}_{23}(h_{23} - h_{25}) = \dot{m}_{33}(h_{34} - h_{33})$	(28)
Recuperator 2	$\dot{m}_{24}(h_{24} - h_{26}) = \dot{m}_{37}(h_{38} - h_{37})$	(29)
Pre-cooler	$\dot{m}_{27}(h_{27} - h_{28}) = \dot{m}_{36}(h_{37} - h_{36})$	(30)
Recuperator 3	$\dot{m}_{28}(h_{28} - h_{29}) = \dot{m}_{32}(h_{33} - h_{32})$	(31)
Expansion valve 1	$h_{36} = h_{35}$	(32)
Expansion valve 2	$h_{30} = h_{29}$	(33)
Separator	$\dot{m}_{30}h_{30} = \dot{m}_{31}h_{31} + \dot{m}_{32}h_{32}$	(34)
Mixer	$\dot{m}_{20}h_{20} + \dot{m}_{34}h_{34} = \dot{m}_{21}h_{21}$	(35)

In the next step, the feasibility of constructing this proposal is studied using by the exergo-economic model. As a robust tool, the exergo-economic provides helpful information about the cost of the system's productions through bridging two common models of exergy and economic. This model is based on the balance of the costs per unit exergy which is written as Eq. (40) for component k [42].

$$\left(\sum\nolimits_{in}\dot{C}_{in,k}\right) + \left(\sum\dot{C}_{Q,k}\right) + \dot{Z}_k = \left(\sum\nolimits_{out}\dot{C}_{out,k}\right) + \left(\sum\dot{C}_{W,k}\right) \quad (40)$$

where, the parameter $\dot{C}_k$ shows the cost rate for component k, which the indices of "in", "out", Q, and W refers to the inlet streams, outlet streams, heat transfer, and power in component k. Also, $\dot{Z}_k$ stands for the rate of capital cost and is defined as follows [43,44]:

$$\dot{Z}_k = \dot{Z}_k^{PEC} + \dot{Z}_k^{O\&M} = PEC_k \times CRC \times \Phi\ ;\ \dot{Z}_{tot} = \sum\nolimits_{all\ components}\dot{Z}_k \quad (41)$$

$$CRC = i_{eff} \times \left[\frac{(1+i_{eff})^N}{(1+i_{eff})^N - 1}\right] \quad (42)$$

where, the parameters of PEC_k, CRC, Φ, i_{eff}, and N denotes the purchasing equipment cost for component k, cost recovery coefficient, operating/maintenance (O&M) factor, rate of effective interest, and system's life span, respectively.

By applying Eq. (40) and simplifying it, the final format of the cost balance equation for all the system components is reported in Table A2 in Appendix A.

As one economical assessment index, the levelized costs of energy of the system under investigation is defined as follows:

$$LCOE = \frac{\dot{Z}_k}{\dot{W}_{net} + \dot{E}x_{Liquid\ hydrogen}} \quad (43)$$

Environmental governing equations

The environmental impacts of the energy systems is another issue which should be addressed in addition to its techno-economic feasibility. Because the global warming phenomenon caused by the greenhouse gases emissions is of the most important international challenges. For this, in many countries, heavy taxes are levied on industries that emit excessive amounts of greenhouse gases. Accordingly, the environmental behavior of the proposed system is assessed by defining the following criterion [45]:

$$\zeta_{CO_2} = \frac{\dot{m}_{CO_2}}{\dot{W}_{net}} \quad (44)$$

Parametric study and optimization procedures

After developing the governing equations, a parametric evaluation is carried out to study the impact of some important design parameters on the objective functions. Here, four design parameters are considered including the biomass flow rate $\dot{m}_{biomass}$, gas turbine inlet temperature T_{GT}, compressor pressure ratio PR, and steam turbine inlet pressure P_{SRCT}. The governing equations are solved through developing a computational program in the EES (Engineering Equation Solver) software.

Afterward, the optimal operating conditions are obtained through a tri-objective robust optimization approach in the MATLAB software (the EES outputs are coupled with MATLAB). The NSGA-II (Non-dominated Sorting Genetic Algorithm), an

Table 3 – Information of the design parameters and objective functions.

Design parameter	Range	
	Lower	Upper
$\dot{m}_{biomass}$ (kg/s)	0.1	2
T_{GT} (K)	1000	1500
PR	5	20
P_{SRCT} (kPa)	2500	5000
Objective function	**Status**	
$\dot{W}_{net}$ (kW)	Should be maximized	
$\dot{m}_{hydrogen}$ (kg/s)	Should be maximized	
$\dot{Z}_{tot}$ ($/h)	Should be minimized	
Specification of the NSGA-II	**Value**	
Generations	300	
Population	1000	
Pareto front population fraction	0.35	
Crossover probability	0.9	

evolutionary optimization tool which provides appropriate results in the field of study [46], is used as the optimization method and the net generated power ($\dot{W}_{net}$), produced liquid hydrogen ($\dot{m}_{hydrogen}$), and total costs rate ($\dot{Z}_{tot}$) are considered as three objective functions. The details of the design parameters and objective functions for the parametric study and optimization procedures are presented in Table 3. It is worth mentioning that the appropriate range of the design parameters is selected relying on the previous published papers and also based on the widest range in which the system operation is thermodynamically possible.

Fig. 2 is drawn for the sake of summarizing different steps of the problem under investigation. This figure gives information about the design, solution, and optimization steps.

Results and discussion

In this section, the efforts are focused on the presentation of the modeling outputs, including the outputs of the parametric sensitivity analysis and optimization process. Before it, the validity of the developed model should be proven.

Validation

The validation of the modeling outputs is proven through the comparison of them with reliable experimental works in the field of study. For this, the outputs of the biomass gasification and PEM electrolyzer are respectively compared with

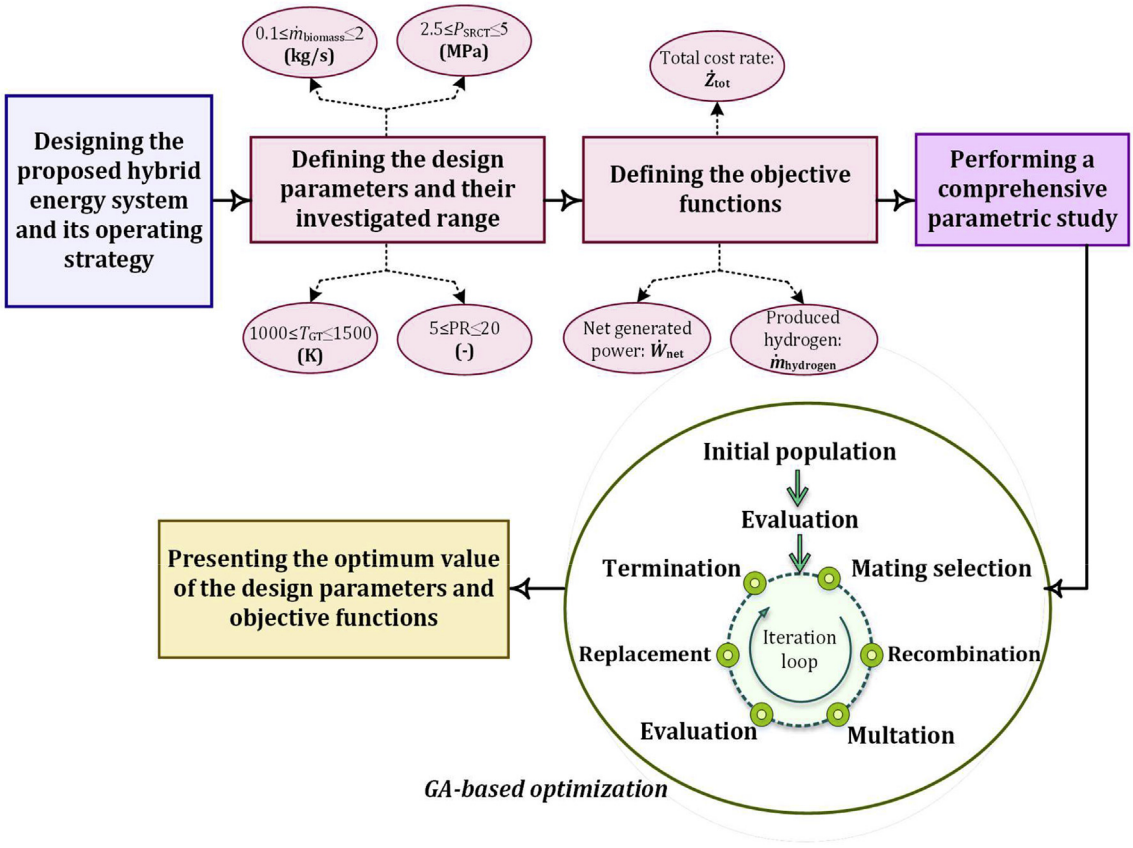

Fig. 2 – Schematic illustration of the problem's different steps.

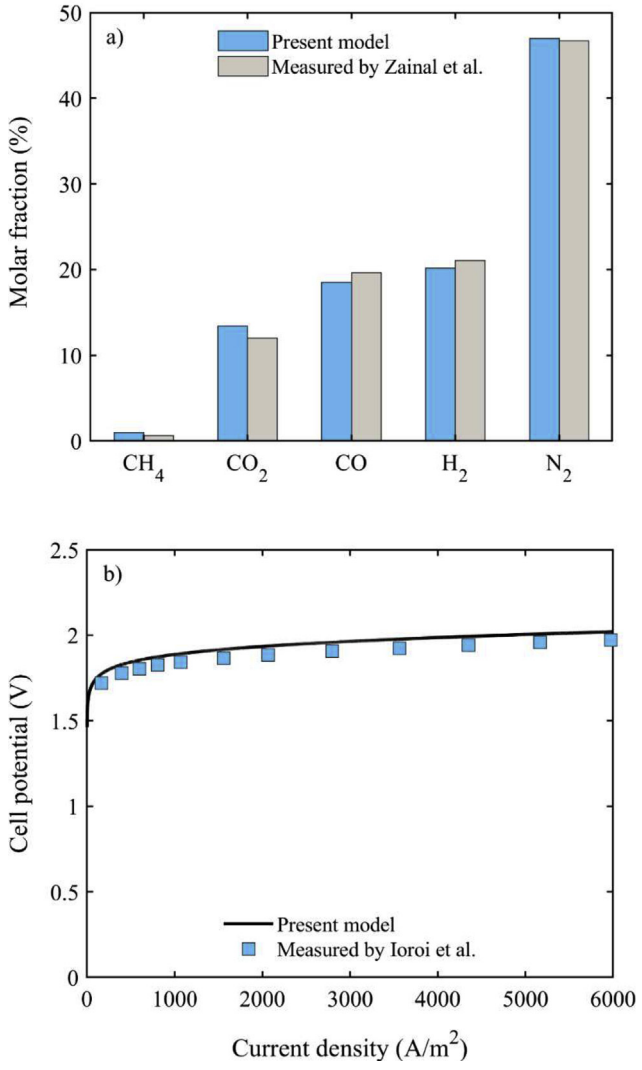

Fig. 3 – Validation of simulation of a) biomass gasification b) PEM electrolyzer.

experiment data of Zainal et al. [47] and Ioroi et al. [48], and the findings of the procedure is drawn in Fig. 3. This figure illustrates that the modeling outputs of this paper are accurate enough.

Parametric study outputs

The effects of biomass mass flow rate on the exergy efficiency, total cost rate, net generated electric power, and produced liquid hydrogen mass flow rate are demonstrated in Fig. 4. It is evident from Fig. 4b that the amount of generated electricity by the system would uniformly rise (with a constant slope) by increasing the biomass mass flow rate due to the higher mass flow rate Brayton cycle (mass flow rate of point 7). This culminates in the need for larger equipment and consequently raised cost rates. In addition, by increasing this parameter, the produced work in SRC also increases, leading to a higher liquid hydrogen mass flow rate.

The input temperature of the gas turbine is one of the most significant parameters in gas turbine cycle design, and the effect of this parameter is represented in Fig. 5. The amount of net generated power by the system will increase by raising the input temperature of the gas turbine due to the higher energy of gases entering the turbine. In general, increasing the input temperature of the gas turbine improves efficiency. However, considering the existing limitations on the material of the turbine blades, it is impossible to raise the temperature over the limit. The cost function will rise with higher slopes by increasing the temperature to values higher than 1450 K.

One of the other essential parameters influencing the performance of the system is the compressor's pressure ratio. Fig. 6 illustrates the analysis of the effects of this parameter on the defined system assessment indices. The temperature of the air entering the combustion chamber is increased by higher pressure ratios leading to raise power in the gas turbine. Moreover, even though higher pressure ratios also increase the compressor's power consumption, the turbine's

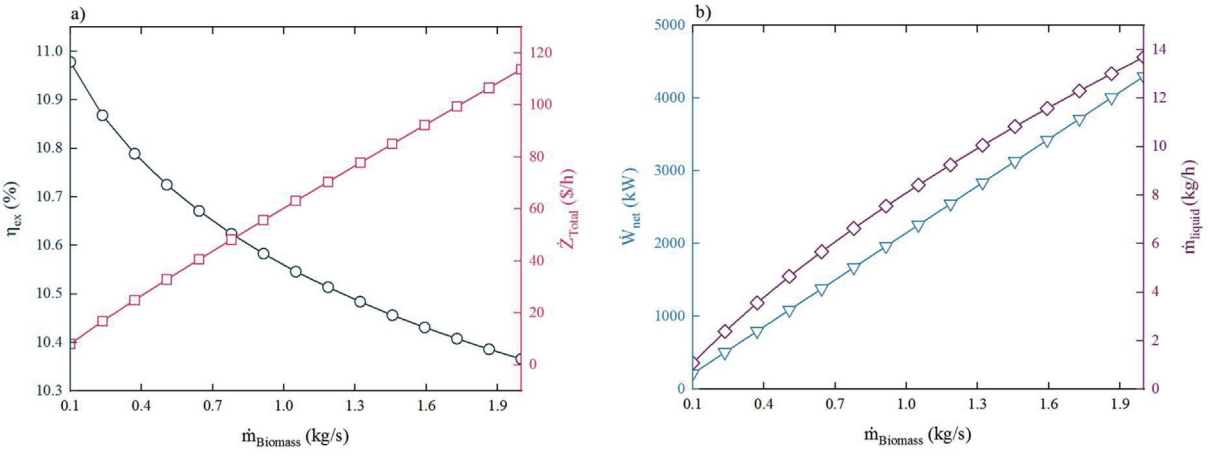

Fig. 4 – Effect of biomass mass flow rate on the, a) exergy efficiency and total cost rate, b) net output power and liquid hydrogen mass flow rate.

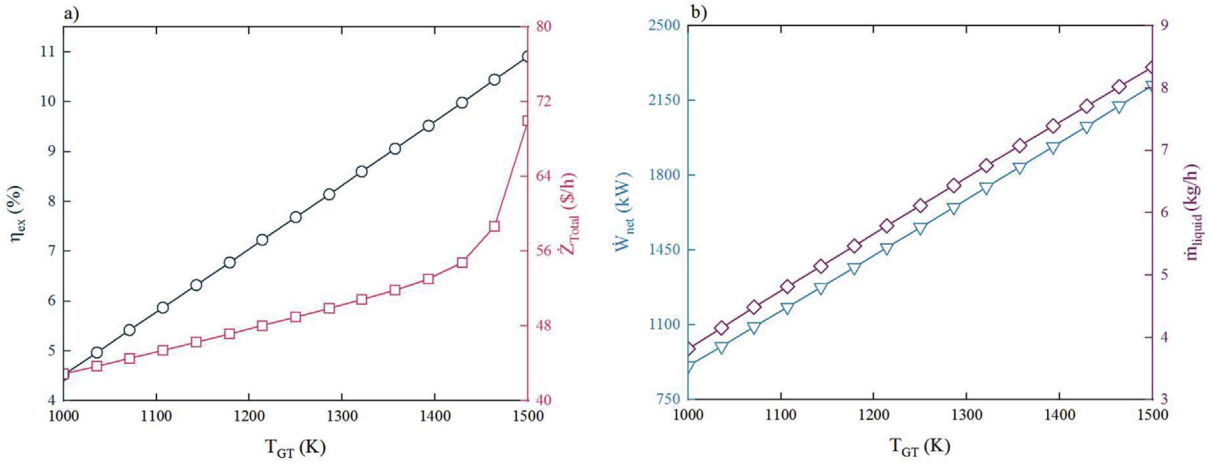

Fig. 5 – Effect of input temperature of the gas turbine on the, a) exergy efficiency and total cost rate, b) net output power and liquid hydrogen mass flow rate.

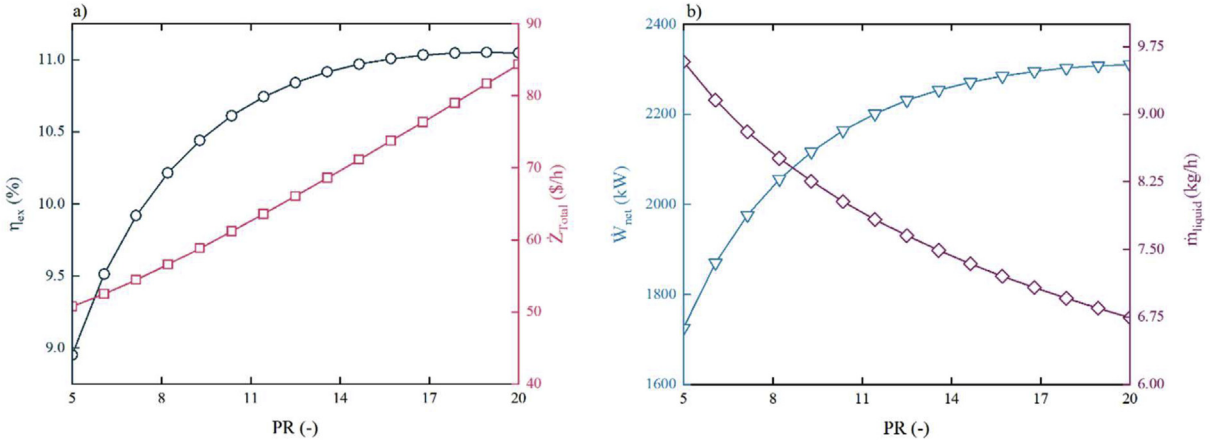

Fig. 6 – Effect of pressure ratio on the a) exergy efficiency and total cost rate b) net output power and liquid hydrogen mass flow rate.

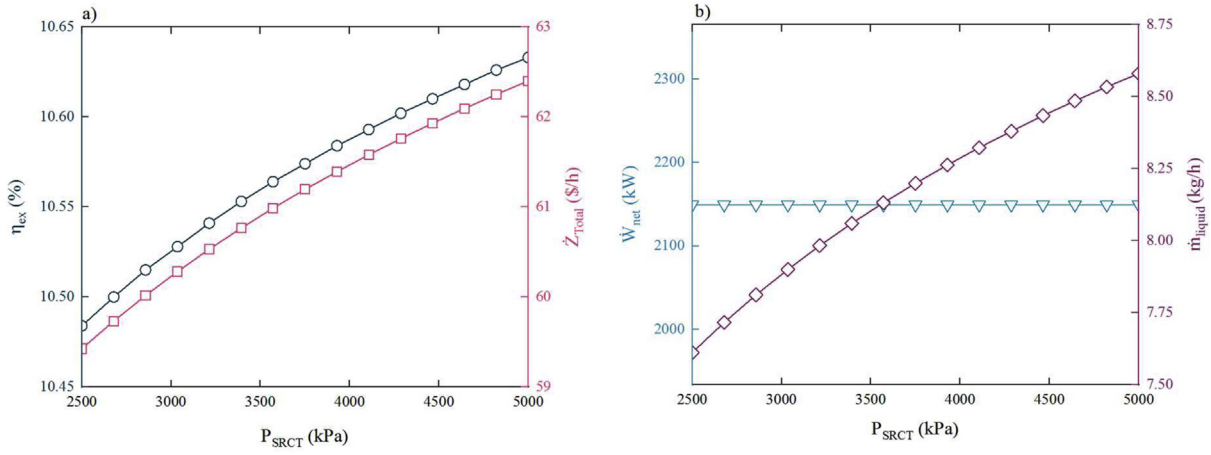

Fig. 7 – Effect of steam turbine's input pressure on the a) exergy efficiency and total cost rate b) net output power and liquid hydrogen mass flow rate.

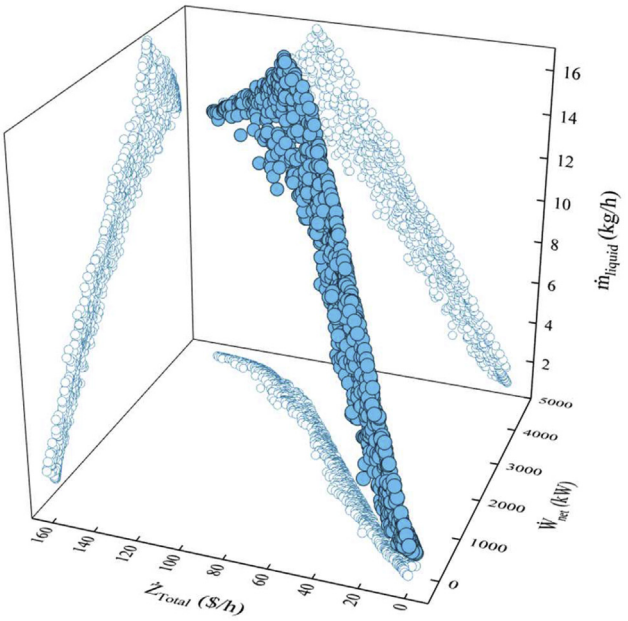

Fig. 8 – Results of all evaluations during 1000 generations using genetic algorithm.

generated power dominates the compressor's power consumption in lower pressure ratios. However, as this value exceeds a specific value, the course will reverse, and the exergy efficiency will be reduced. In addition, higher pressure ratios increase the costs of the compressor and other utilities,

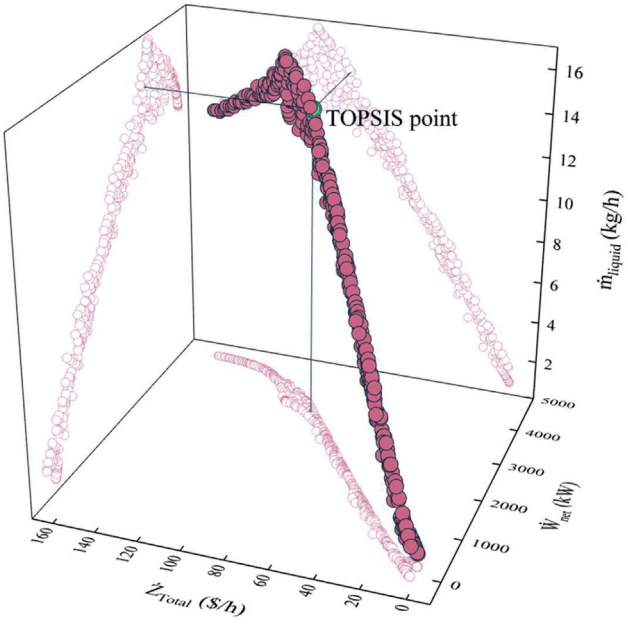

Fig. 9 – Pareto frontier of the net output power, liquid hydrogen mass flow rate, and total cost rate as a result of tri-objective optimization.

Table 4 – Objective functions and decision variable values for TOPSIS point.

Item	Parameter	Value
Design parameters	$\dot{m}_{Biomass}$ (kg/s)	1.94
	T_{GT} (K)	1421
	PR (–)	5.52
	P_{SRCT} (kPa)	3886
Objective functions	$\dot{W}_{net}$ (kW)	3377
	$\dot{Z}_{tot}$ ($/h)	86.61
	$\dot{m}_{Hydrogen}$ (kg/h)	14.80
Important results	η_{ex} (%)	10.52
	ζ_{CO_2} (kg/kWh)	1.09
	LCOE ($/MWh)	26.3

resulting in an increased total cost rate of the system. By raising the pressure ratio, the mass flow rate in the Brayton cycle and resultantly in SRC decreases, leading to lower generated electricity in SRC and lower liquid hydrogen discharge production.

The effects of variations of the steam turbine's input pressure on the system's important outputs are demonstrated in Fig. 7. By increasing the input pressure of the steam turbine, the input enthalpy of the turbine is grown, which increases the SRC power and produced hydrogen. However, the net output power is not altered since the whole power of the SRC is transferred into the liquefaction unit.

Optimization outputs

The outputs of the described three-objective optimization is conducted in this section. Fig. 8 shows the three-dimensional diagram for 1000 population. The Pareto optimal frontier, which selects the points with the best rank, is represented in Fig. 9 separately to have a better selection. In addition, the best point chosen by the TOPSIS decision-making scale is illustrated in Fig. 9. The TOPSIS method is a standard technique in multi-objective decision-making. According to this method, numerous options and goals must be ranked based on optimal points, their objective functions, or each one needs to be ranked according to its performance value. In the TOPSIS method, the criteria for calculating the order of optimal points is that options should be as close as possible to the ideal option while as far away as possible from the ideal negative option [49].

As the optimal values for each objective function in TOPSIS point, the net output power is 3377 kW, the liquid hydrogen mass flow rate is 14.80 kg/h, and the total cost rate is 86.61 $/h. The optimization functions and variables for the TOPSIS point are depicted in Table 4.

The scatter distribution for the investigated design parameters is demonstrated in Fig. 10. It is evident that all optimal parameters for the input temperature of the gas turbine are set to their maximal limit. This performance was anticipated according to the results represented in Fig. 5. Moreover, most of the optimal points for pressure ratio are from 5 to 8.

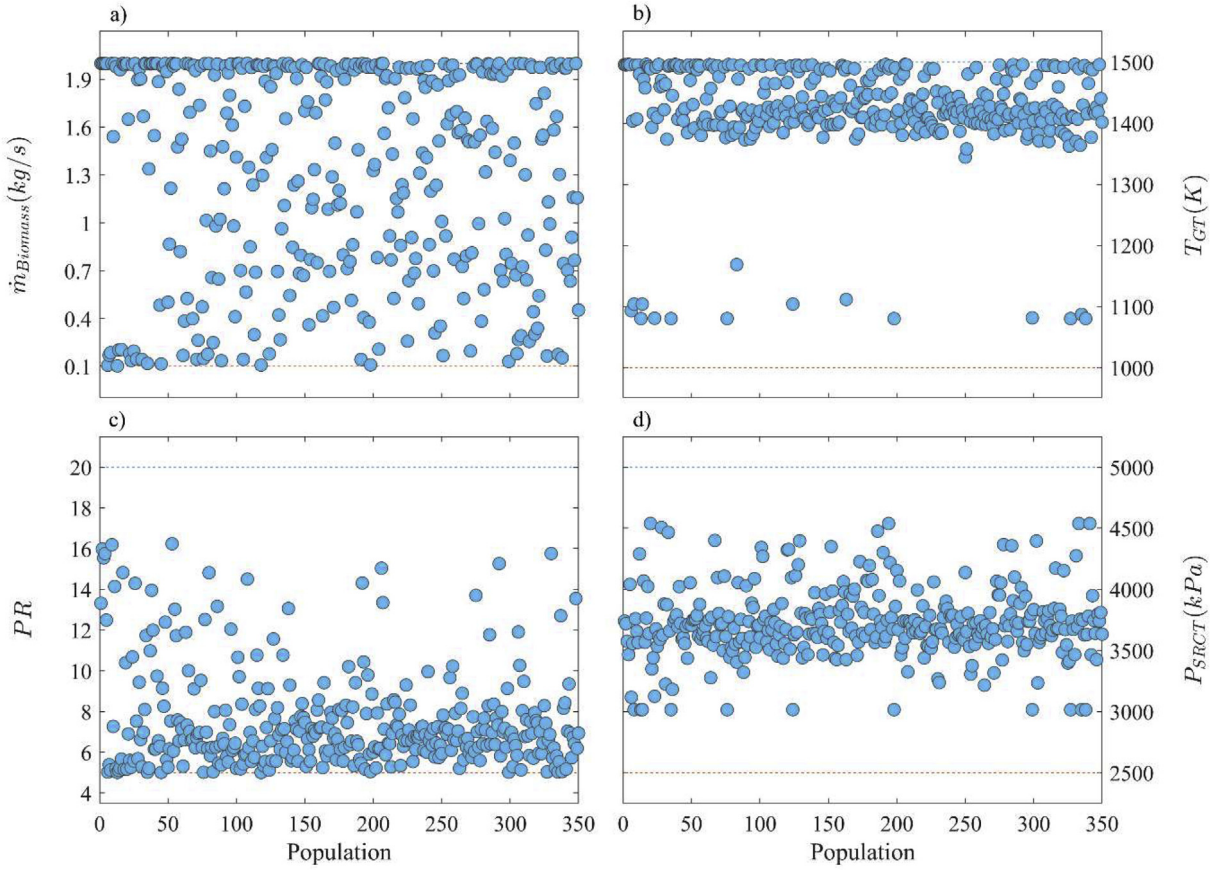

Fig. 10 – Scattered distribution of decision variables with population in Pareto frontier.

Conclusion

Designing new configurations of HPPs based on the combination conventional thermodynamic cycles has become a vital issue to have cleaner productions and stable grid, and reach sustainably goals. Consequently, in this study, a new power and liquid hydrogen HPP is introduced which comprises a biomass gasification gas turbine cycle, a Rankine cycle, an electrolyzer unit, and a hydrogen liquefaction cycle. A potent techno-economic-environmental parametric model was built to evaluate the construction possibility of the system.

After developing the governing equations, the effect of changing the biomass flow rate $\dot{m}_{biomass}$, gas turbine inlet temperature T_{GT}, compressor pressure ratio PR, and steam turbine inlet pressure P_{SRCT} was studied on the defined performance criteria. The outputs of this sensitivity analysis revealed that the mass flow rate of the biomass is the most effective design parameter.

At the second step, the optimal design parameters and the corresponding value of the objective functions is selected using by a multi-objective optimization approach. Applying this procedure, the optimal design parameters are obtained as $\dot{m}_{biomass}$ = 1.94 kg/s, T_{GT} = 1421 K, PR = 5.52, and P_{SRCT} = 3886 kPa, which results in the maximum electricity and hydrogen production of 3377 kW and 14.8 kg/h together with minimum total cost rate of 86.61 $/h. At this condition, the optimal environmental index is 1.09 kg_{CO_2}/kWh.

In this paper, the technical, economic, and environmental feasibility of constructing the introduced HPP was demonstrated. As some suggestions for future papers on this system, the following items can be done: (1) Advanced exergy and exergoeconomic analyses. These analyses presents a deeper understanding from technical and economic points-of-view. (2) Evaluating various methods to improve the environmental condition of the GTC which makes this proposal even more enviro-friendly. For example, injecting the vapor into combustion chamber and utilizing intercooler and preheater may be helpful.

Declaration of competing interest

The authors declare that they have no known competing financial interests or personal relationships that could have appeared to influence the work reported in this paper.

Acknowledgement

The authors extend their appreciation to the Deanship of Scientific Research at King Khalid University for funding this work through research groups under grant number R.G.P.2/14/43.

Appendix A. Supplementary data

Supplementary data to this article can be found online at https://doi.org/10.1016/j.ijhydene.2022.01.110.

REFERENCES

[1] Li B, Xiao G, Lu R, Deng R, Bao H. On feasibility and limitations of detecting false data injection attacks on power grid state estimation using D-FACTS devices. IEEE Trans Ind Inf 2020;16:854–64. https://doi.org/10.1109/TII.2019.2922215.

[2] Xu X, Wang C, Zhou P. GVRP considered oil-gas recovery in refined oil distribution: from an environmental perspective. Int J Prod Econ 2021;235:108078. https://doi.org/10.1016/j.ijpe.2021.108078.

[3] Deng W, Xu K, Xiong Z, Chaiwat W, Wang X, Su S, et al. Evolution of aromatic structures during the low-temperature electrochemical upgrading of bio-oil. Energy Fuels 2019;33:11292–301. https://doi.org/10.1021/acs.energyfuels.9b03099.

[4] Farzaneh-Gord M, Pahlevan-Zadeh MS, Ebrahimi-Moghadam A, Rastgar S. Measurement of methane emission into environment during natural gas purging process. Environ Pollut 2018;242:2014–26. https://doi.org/10.1016/j.envpol.2018.07.027.

[5] Wang T, Liu W, Zhao J, Guo X, Terzija V. A rough set-based bio-inspired fault diagnosis method for electrical substations. Int J Electr Power Energy Syst 2020;119:105961. https://doi.org/10.1016/j.ijepes.2020.105961.

[6] Shen Z, Wang F, Wang Z, Li J. A critical review of plant-based insulating fluids for transformer: 30-year development. Renew Sustain Energy Rev 2021;141:110783. https://doi.org/10.1016/j.rser.2021.110783.

[7] Hu Z, Zhang L, Huang J, Feng Z, Xiong Q, Ye Z, et al. Self-supported nickel-doped molybdenum carbide nanoflower clusters on carbon fiber paper for an efficient hydrogen evolution reaction. Nanoscale 2021;13:8264–74. https://doi.org/10.1039/D1NR00169H.

[8] Zhang T, Wu X, Shaheen SM, Abdelrahman H, Ali EF, Bolan NS, et al. Improving the humification and phosphorus flow during swine manure composting: a trial for enhancing the beneficial applications of hazardous biowastes. J Hazard Mater 2022;425:127906. https://doi.org/10.1016/j.jhazmat.2021.127906.

[9] Alirahmi SM, Mousavi SF, Ahmadi P, Arabkoohsar A. Soft computing analysis of a compressed air energy storage and SOFC system via different artificial neural network architecture and tri-objective grey wolf optimization. Energy 2021;236:121412. https://doi.org/10.1016/j.energy.2021.121412.

[10] Habibollahzade A, Gholamian E, Ahmadi P, Behzadi A. Multi-criteria optimization of an integrated energy system with thermoelectric generator, parabolic trough solar collector and electrolysis for hydrogen production. Int J Hydrogen Energy 2018;43:14140–57. https://doi.org/10.1016/j.ijhydene.2018.05.143.

[11] Deymi-Dashtebayaz M, Ebrahimi-Moghadam A, Pishbin SI, Pourramezan M. Investigating the effect of hydrogen injection on natural gas thermo-physical properties with various compositions. Energy 2019;167:235–45. https://doi.org/10.1016/j.energy.2018.10.186.

[12] Okati V, Ebrahimi-Moghadam A, Behzadmehr A, Farzaneh-Gord M. Proposal and assessment of a novel hybrid system for water desalination using solar and geothermal energy sources. Desalination 2019;467:229–44. https://doi.org/10.1016/j.desal.2019.06.011.

[13] Wang A, Wang S, Ebrahimi-Moghadam A, Farzaneh-Gord M, Moghadam AJ. Techno-economic and techno-environmental assessment and multi-objective optimization of a new CCHP system based on waste heat recovery from regenerative Brayton cycle. Energy 2021:122521. https://doi.org/10.1016/j.energy.2021.122521.

[14] Ebrahimi-Moghadam A, Farzaneh-Gord M. Energy, exergy, and eco-environment modeling of proton exchange membrane electrolyzer coupled with power cycles: application in natural gas pressure reduction stations. J Power Sources 2021;512:230490. https://doi.org/10.1016/j.jpowsour.2021.230490.

[15] Ebrahimi-Moghadam A, Farzaneh-Grod M. Optimal operation of a multi-generation district energy hub based on electrical, heating, and cooling demands and hydrogen production. Appl Energy 2022.

[16] Altinkaynak M, Ozturk M. Thermodynamic analysis of a novel integrated system operating with gas turbine, s-CO2 and t-CO2 power systems for hydrogen production and storage. Int J Hydrogen Energy 2021. https://doi.org/10.1016/j.ijhydene.2021.07.212.

[17] Ebrahimi-Moghadam A, Farzaneh-Gord M, Jabari Moghadam A, Abu-Hamdeh NH, Lasemi MA, Arabkoohsar A, et al. Design and multi-criteria optimisation of a trigeneration district energy system based on gas turbine, Kalina, and ejector cycles: exergoeconomic and exergoenvironmental evaluation. Energy Convers Manag 2021;227:113581. https://doi.org/10.1016/j.enconman.2020.113581.

[18] Ding P, Liu X, Qi H, Shen H, Liu X, Farkoush SG. Multi-objective optimization of a new cogeneration system driven by gas turbine cycle for power and freshwater production. J Clean Prod 2021;288:125639. https://doi.org/10.1016/j.jclepro.2020.125639.

[19] Ahmadi P, Khanmohammadi S, Musharavati F, Afrand M. Development, evaluation, and multi-objective optimization of a multi-effect desalination unit integrated with a gas turbine plant. Appl Therm Eng 2020;176:115414. https://doi.org/10.1016/j.applthermaleng.2020.115414.

[20] Ebrahimi-Moghadam A, Jabari Moghadam A, Farzaneh-Gord M, Arabkoohsar A. Performance investigation of a novel hybrid system for simultaneous production of cooling, heating, and electricity. Sustain Energy Technol Assessments 2021;43:100931. https://doi.org/10.1016/j.seta.2020.100931.

[21] Alirahmi SM, Razmi AR, Arabkoohsar A. Comprehensive assessment and multi-objective optimization of a green concept based on a combination of hydrogen and compressed air energy storage (CAES) systems. Renew Sustain Energy Rev 2021;142:110850. https://doi.org/10.1016/j.rser.2021.110850.

[22] Al-Hamed KHM, Dincer I. A new solar energy-based integrated carbon capturing system with a gas turbine-supercritical CO2 combined power cycle. Energy Convers Manag 2022;251:114999. https://doi.org/10.1016/j.enconman.2021.114999.

[23] Musharavati F, Khoshnevisan A, Alirahmi SM, Ahmadi P, Khanmohammadi S. Multi-objective optimization of a biomass gasification to generate electricity and desalinated water using Grey Wolf Optimizer and artificial neural network. Chemosphere 2022;287:131980. https://doi.org/10.1016/j.chemosphere.2021.131980.

[24] Cao Y, Dhahad HA, Togun H, Anqi AE, Farouk N, Farhang B. A novel hybrid biomass-solar driven triple combined power cycle integrated with hydrogen production: multi-objective optimization based on power cost and CO2 emission. Energy Convers Manag 2021;234:113910. https://doi.org/10.1016/j.enconman.2021.113910.

[25] Alirahmi SM, Khoshnevisan A, Shirazi P, Ahmadi P, Kari D. Soft computing based optimization of a novel solar heliostat integrated energy system using artificial neural networks. Sustain Energy Technol Assessments 2022;50:101850. https://doi.org/10.1016/j.seta.2021.101850.
[26] Wang J, Lu Z, Li M, Lior N, Li W. Energy, exergy, exergoeconomic and environmental (4E) analysis of a distributed generation solar-assisted CCHP (combined cooling, heating and power) gas turbine system. Energy 2019;175:1246–58. https://doi.org/10.1016/j.energy.2019.03.147.
[27] Karimi MH, Chitgar N, Emadi MA, Ahmadi P, Rosen MA. Performance assessment and optimization of a biomass-based solid oxide fuel cell and micro gas turbine system integrated with an organic Rankine cycle. Int J Hydrogen Energy 2020;45:6262–77. https://doi.org/10.1016/j.ijhydene.2019.12.143.
[28] Nazari N, Porkhial S. Multi-objective optimization and exergo-economic assessment of a solar-biomass multi-generation system based on externally-fired gas turbine, steam and organic Rankine cycle, absorption chiller and multi-effect desalination. Appl Therm Eng 2020;179:115521. https://doi.org/10.1016/j.applthermaleng.2020.115521.
[29] Shokouhi Tabrizi AH, Niazmand H, Farzaneh-Gord M, Ebrahimi-Moghadam A. Energy, exergy and economic analysis of utilizing the supercritical CO2 recompression Brayton cycle integrated with solar energy in natural gas city gate station. J Therm Anal Calorim 2021;145:973–91. https://doi.org/10.1007/s10973-020-10241-9.
[30] Aghbashlo M, Rastegari H, Ghaziaskar HS, Hosseinzadeh-Bandbafha H, Nadian MH, Shafizadeh A, et al. Exergy, economic, and environmental assessment of ethanol dehydration to diesel fuel additive diethyl ether. Fuel 2022;308:121918. https://doi.org/10.1016/j.fuel.2021.121918.
[31] Ishaq H, Islam S, Dincer I, Yilbas BS. Development and performance investigation of a biomass gasification based integrated system with thermoelectric generators. J Clean Prod 2020;256:120625. https://doi.org/10.1016/j.jclepro.2020.120625.
[32] Martínez González A, Lesme Jaén R, Silva Lora EE. Thermodynamic assessment of the integrated gasification-power plant operating in the sawmill industry: an energy and exergy analysis. Renew Energy 2020;147:1151–63. https://doi.org/10.1016/j.renene.2019.09.045.
[33] Fakhari I, Behzadi A, Gholamian E, Ahmadi P, Arabkoohsar A. Design and tri-objective optimization of a hybrid efficient energy system for tri-generation, based on PEM fuel cell and MED using syngas as a fuel. J Clean Prod 2021;290:125205. https://doi.org/10.1016/j.jclepro.2020.125205.
[34] Habibollahzade A, Ahmadi P, Rosen MA. Biomass gasification using various gasification agents: optimum feedstock selection, detailed numerical analyses and tri-objective grey wolf optimization. J Clean Prod 2021;284:124718. https://doi.org/10.1016/j.jclepro.2020.124718.
[35] Alirahmi SM, Assareh E, Chitsaz A, Ghazanfari Holagh S, Jalilinasrabady S. Electrolyzer-fuel cell combination for grid peak load management in a geothermal power plant: power to hydrogen and hydrogen to power conversion. Int J Hydrogen Energy 2021;46:25650–65. https://doi.org/10.1016/j.ijhydene.2021.05.082.
[36] Alirahmi SM, Assareh E. Energy, exergy, and exergoeconomics (3E) analysis and multi-objective optimization of a multi-generation energy system for day and night time power generation - case study: dezful city. Int J Hydrogen Energy 2020;45:31555–73. https://doi.org/10.1016/j.ijhydene.2020.08.160.
[37] Sattari Sadat SM, Ghaebi H, Lavasani AM. 4E analyses of an innovative polygeneration system based on SOFC. Renew Energy 2020;156:986–1007. https://doi.org/10.1016/j.renene.2020.04.139.
[38] Dincer I, Rosen MA, Ahmadi P. Modeling and optimization of multigeneration energy systems. Optim. Energy Syst. 2017:398–446. https://doi.org/10.1002/9781118894484.ch11.
[39] Alirahmi SM, Rahmani Dabbagh S, Ahmadi P, Wongwises S. Multi-objective design optimization of a multi-generation energy system based on geothermal and solar energy. Energy Convers Manag 2020;205:112426. https://doi.org/10.1016/j.enconman.2019.112426.
[40] Ebrahimi-Moghadam A, Deymi-Dashtebayaz M, Jafari H, Niazmand A. Energetic, exergetic, environmental and economic assessment of a novel control system for indirect heaters in natural gas city gate stations. J Therm Anal Calorim 2020;141:2573–88. https://doi.org/10.1007/s10973-020-09413-4.
[41] Ebrahimi-Moghadam A, Moghadam AJ, Farzaneh-Gord M, Aliakbari K. Proposal and assessment of a novel combined heat and power system: energy, exergy, environmental and economic analysis. Energy Convers Manag 2020;204:112307. https://doi.org/10.1016/j.enconman.2019.112307.
[42] Alirahmi SM, Bashiri Mousavi S, Razmi AR, Ahmadi P. A comprehensive techno-economic analysis and multi-criteria optimization of a compressed air energy storage (CAES) hybridized with solar and desalination units. Energy Convers Manag 2021;236:114053. https://doi.org/10.1016/j.enconman.2021.114053.
[43] Ebrahimi-Moghadam A, Moghadam AJ, Farzaneh-Gord M. Comprehensive techno-economic and environmental sensitivity analysis and multi-objective optimization of a novel heat and power system for natural gas city gate stations. J Clean Prod 2020;262:121261. https://doi.org/10.1016/j.jclepro.2020.121261.
[44] Alirahmi SM, Assareh E, Pourghassab NN, Delpisheh M, Barelli L, Baldinelli A. Green hydrogen & electricity production via geothermal-driven multi-generation system: thermodynamic modeling and optimization. Fuel 2022;308:122049. https://doi.org/10.1016/j.fuel.2021.122049.
[45] Sikarwar SS, Surywanshi GD, Patnaikuni VS, Kakunuri M, Vooradi R. Chemical looping combustion integrated Organic Rankine Cycled biomass-fired power plant – energy and exergy analyses. Renew Energy 2020;155:931–49. https://doi.org/10.1016/j.renene.2020.03.114.
[46] Ebrahimi-Moghadam A, Kowsari S, Farhadi F, Deymi-Dashtebayaz M. Thermohydraulic sensitivity analysis and multi-objective optimization of Fe3O4/H2O nanofluid flow inside U-bend heat exchangers with longitudinal strip inserts. Appl Therm Eng 2020;164:114518. https://doi.org/10.1016/j.applthermaleng.2019.114518.
[47] Zainal ZA, Ali R, Lean CH, Seetharamu KN. Prediction of performance of a downdraft gasifier using equilibrium modeling for different biomass materials. Energy Convers Manag 2001;42:1499–515. https://doi.org/10.1016/S0196-8904(00)00078-9.
[48] Ioroi T, Yasuda K, Siroma Z, Fujiwara N, Miyazaki Y. Thin film electrocatalyst layer for unitized regenerative polymer electrolyte fuel cells. J Power Sources 2002;112:583–7. https://doi.org/10.1016/S0378-7753(02)00466-4.
[49] Assareh E, Alirahmi SM, Ahmadi P. A Sustainable model for the integration of solar and geothermal energy boosted with thermoelectric generators (TEGs) for electricity, cooling and desalination purpose. Geothermics 2021;92:102042. https://doi.org/10.1016/j.geothermics.2021.102042.